XVI. CHEMICAL COMPOSITION OF SEDIMENT CORES FROM THE GH79-1 AREA

*David Z. Piper**

Introduction

Sediment samples from three box cores and one piston core, collected on cruise GH79–1 of the research vessel Hakurei-Maru, were analyzed for major oxides and minor elements. All cores were collected from a small area of the Central Pacific Ocean, centered at 167°40'W and 10°N (Fig. XVI-1). Forty-four samples were leached with hydroxylamine hydrochloride-acetic acid (HHCl-HAc) and the soluble fraction of 12 elements (Si, Al, Ca, Mg, K, Na, Fe, Mn, Co, Ni, and Zn) measured. The concentrations of 10 elements (Si, Al, Fe, Mg, Ca, Na, K, Ti, P, and Mn) were determined for 15 bulk sediment samples and 5 samples of the sediment fraction insoluble in HHCl-Ac.

The fine fraction (grain size less than approximately 5 μm) of pelagic sediments consists of a mixture of sedimentary components classified according to their origin as hydrogenous, biogenous and lithogenous (GOLDBERG, 1963). From the bulk chemical analyses I calculate that the concentration of the biogenic phases, opaline silica and $CaCO_3$,
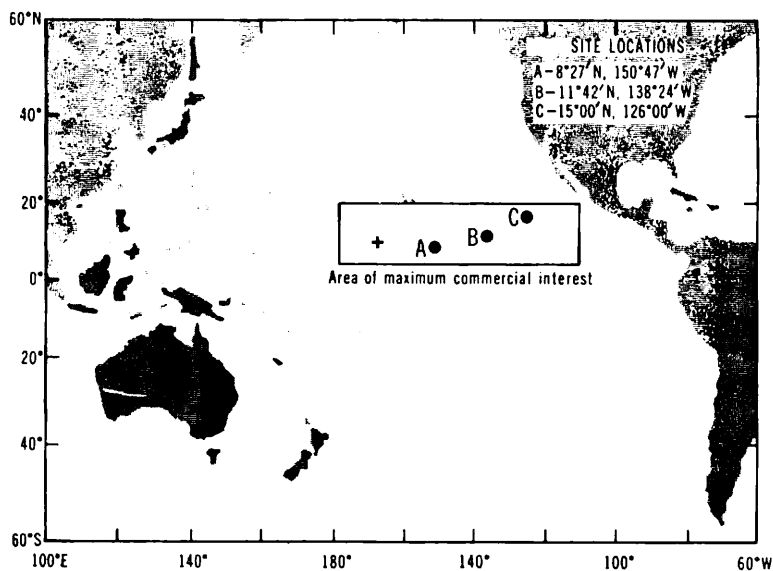

Fig. XVI-1 Location of the area surveyed in this study (shown by +) and of the three DOMES sites. Location of the DOMES sites are given in the upper right corner. For the latitude and longitude of the area of the Central Pacific Basin examined in this study see other papers in this cruise report.

*U.S. Geological Survey, Menlo Park, U.S.A

varies between 3 and 53% but averages 10%. The insoluble residue is interpreted to consist of lithogenic material, whose composition is well defined by its metal:Al_2O_3 ratios, and opaline silica. The soluble fraction may represent the hydrogenous component, which consists of exchangeable ions and amorphous metal oxides (largely of Fe, Mn, and possibly Al). Ca^{++}, as $CaCO_3$, is also present in this fraction.

The aim of this study is to ascertain the relation between the composition of these components and the composition and abundance of associated manganese nodules.

Technique

The major oxides were measured by X-ray fluorescence. The composition of the soluble fraction of sediment was measured by atomic absorption after leaching the sediment samples, following the method of CHESTER and HUGHES (1967), at a temperature of 20°C. Accuracy and precision for the X-ray fluorescence analyses are better than 1% and, for the atomic absorption analyses, they are approximately 5%. The results of these analyses are given in Tables XVI-1 and -2.

Bulk Sediment Composition

The bulk sediment consists of lithogenic matter, which may be terrigenous or marine in origin; biogenic material (opaline silica, $CaCO_3$, and minor amounts of hydrocarbons); and hydrogenous material, usually making up approximately 10% of the total sediment and composed mostly of exchangeable ions and amorphous oxides of Fe and Mn. The relative abundances of opaline silica can be estimated by inferring a fixed SiO_2:Al_2O_3 ratio of 3.57 for the lithogenic fraction and assigning the excess SiO_2 to biogenic SiO_2. This value is based on the SiO_2:Al_2O_3 ratio (1) measured on pelagic sediment which is free of biogenic silica (PIPER et al., 1979) and (2) reported for terrigenous shale (Table XVI-3) by TUREKIAN and WEDEPOHL (1961). This "excess" SiO_2 varies between 1.26 and 31.84% (Table XVI-4).

The concentration of $CaCO_3$ can be calculated in the same way, assuming a CaO:Al_2O_3 ratio for the lithogenic component of 0.065 (Table XVI-3). This calculation makes no allowance for the occurrence of Ca^{++} as a surface adsorbed ion. This uncertainty will be partially canceled by the occurrence of some of the Al_2O_3 within the hydrogenous fraction. The uncertainty in the calculation is probably less than 10%. As these samples were collected at depths below the carbonate compensation depth (CCD), they quite expectedly have low $CaCO_3$. Two subsurface samples from piston core P138, however, have high $CaCO_3$ (Table XVI-4).

The hydrogenous component, exclusive of $CaCO_3$, has an average concentration of approximately 6% when each of the metals is expressed as an oxide.

Insoluble Sediment Fraction (ISF)

The insoluble sediment fraction consists of lithogenic material and opaline silica, both of which are not attacked by HHCl-HAc. The concentrations of SiO_2 and TiO_2 changed by less than 2% upon treatment with HHCl-HAc. X-ray diffraction patterns of treated and untreated samples were identical.

Sediment from three other areas has been examined (PIPER et al., 1979) in greater detail than sediment from the area examined in this study. These sites lie along an

Table XVI-1 Bulk chemical composition percent of pelagic sediment samples from the Central Pacific Basin, GH 79-1 detailed survey area. Sample numbers give station and depth in cm. below the surface. The "R" notation of five of the samples refers to these samples as insoluble residues upon treatment with HHCl-HAc. The difference between the totals and 100% represents loss-on-ignition, mostly H_2O and CO_2. Analyses were made by X-ray fluorescence.

Station, position, and bathymetric data of samples

Sample No.	Station	Position		Depth
1481A2	P138	09°59.21'N	167°47.38'W	5270 m
1481	G(B')948	10°01.367N	167°48.83'W	5280 m
1483	G(B)950	09°49.64'N	167°38.99'W	5211 m
1484	G(B')951	09°59.48'N	167°39.60'W	5244 m

	P138 (0-2)	P138 (6-8)	P138 (15-17)	(263-265)	P138 (378-380)	G(B')948 (0-1)	G(B')948 (6-8)	G(B')948 (13-15)	G(B')948 (28-30)	G(B)950 (0-2)
SiO_2	57.59	55.72	56.17	49.94	58.44	58.02	57.24	52.39	53.06	57.39
Al_2O_3	13.40	13.86	13.76	11.10	7.45	12.95	13.13	12.51	14.51	12.98
Fe_2O_3	7.51	7.80	7.56	7.25	4.80	7.49	7.52	7.68	8.38	7.63
MgO	2.90	3.01	2.97	3.73	2.59	2.82	2.86	2.80	3.31	2.86
CaO	1.94	2.02	1.96	5.28	12.17	1.74	1.83	1.67	1.77	1.89
Na_2O	1.38	1.56	1.57	1.32	0.58	1.62	1.60	1.53	1.61	1.57
K_2O	2.90	2.97	2.96	2.47	1.27	2.75	2.89	2.80	3.10	2.82
TiO_2	0.95	0.96	0.94	0.65	0.37	0.86	0.91	0.84	0.91	0.86
P_2O_5	0.49	0.52	0.50	2.26	1.11	0.44	0.46	0.41	0.43	0.50
MnO	1.030	0.984	1.050	1.720	0.906	0.881	0.918	0.839	1.020	0.991
Total	90.09	89.49	89.44	83.72	89.69	89.57	89.36	83.47	88.10	89.49

	G(B')951 (0-2)	G(B')951 (4-6)	G(B')951 (8-10)	G(B')951 (13-15)	G(B')951 (23-25)	P138 (15-17)R	P138 (378-380)R	G(B')948 (13-15)R	G(B')951 (4-6)R	G(B')951 (13-15)R
SiO_2	58.34	60.55	61.77	58.88	54.17	59.76	72.50	59.64	64.06	62.45
Al_2O_3	12.38	12.41	12.26	12.48	13.40	13.76	9.05	13.73	12.22	12.44
Fe_2O_3	7.64	7.50	7.28	7.62	8.11	7.77	5.61	8.28	7.82	7.83
MgO	2.83	2.79	2.70	2.75	2.98	2.72	2.42	2.86	2.55	2.57
CaO	1.62	1.54	1.55	1.60	1.95	0.95	1.06	0.89	0.78	0.77
Na_2O	1.60	1.70	1.48	1.81	1.74	0.92	0.57	0.84	0.77	0.81
K_2O	2.69	2.70	2.67	2.77	2.94	2.49	1.14	2.50	2.28	2.30
TiO_2	0.82	0.82	0.82	0.84	0.93	1.01	0.47	0.97	0.89	0.91
P_2O_5	0.39	0.36	0.38	0.37	0.48	0.07	0.12	0.08	0.08	0.07
MnO	0.876	0.840	0.760	0.765	1.050	0.070	0.055	0.069	0.073	0.066
Total	89.19	91.21	91.67	89.89	87.75	89.52	93.00	89.86	91.52	90.22

Table XVI-2　Elemental composition of the fraction of sediment soluble in HHCl-HAc. Concentrations are in ppm of bulk sediment. All analyses were made by atomic absorption.

Sample No.	Depth (cm)	Al	Si	Ca	Mg	K	Na	Cu	Ni	Co	Zn	Mn	Fe
P138	0-2	6244	1731	8792	7826	9991	8159	193	111	109	187	6660	3930
"	5-8	6372	1953	8576	7266	6479	7266	179	105	103	56	7147	4431
"	25-27	5097	1522	7993	4690	6090	7884	189	111	110	42	6852	3806
"	35-40	5286	1642	7611	4795	6169	8457	145	80	91	26	5025	3383
"	75-80	3315	1601	8606	4253	6305	8106	98	132	113	27	8006	3803
"	145-150	2952	1357	8592	4773	6834	9145	99	134	119	25	10050	3266
"	240-245	2250	1150	21500	4625	11500	12900	179	133	136	42	10000	3250
"	260-265	2892	1851	38570	7328	9462	9128	201	220	138	126	13885	4217
"	310-320	3739	1446	27921	5860	7279	9872	169	182	115	67	10969	3391
"	330-337	125	350	350000	1781	2400	3800	31	36	25	11	1550	1200
"	340-350	1248	1048	167265	3058	4593	6790	85	81	58	24	5243	2397
"	370-380	2795	1234	94164	3183	5248	7503	96	78	71	22	6535	3036
G(B')948	0-2	7695	1910	7483	3947	6156	8226	184	98	96	165	5785	3874
"	2-4	7762	1788	7154	3726	6259	9837	173	91	89	21	5316	3676
"	4-6	7329	1739	7255	3913	6360	9043	172	91	91	26	5317	3876
"	6-8	6702	1819	7624	3596	6099	7378	185	102	104	130	5952	3591
"	8-10	6256	1551	7807	4126	6306	9509	163	91	89	58	5355	3453
"	10-12	6138	1604	7666	4071	6514	11024	157	85	97	150	5612	3658
"	12-15	6339	1775	6897	3169	5781	8114	155	83	96	22	5600	3246
"	15-20	—	1700	7150	3968	6800	10800	155	88	102	24	5750	3950
"	20-25	5097	1840	7260	3978	6564	12333	157	108	101	56	6664	4028
"	25-30	5042	1743	6922	3548	5776	7719	147	108	106	97	6972	4133
"	30-35	4625	1700	7400	4000	6200	9400	126	123	101	165	6550	4050
G(B)950	0-2	7146	1889	8284	4451	6104	7751	197	112	99	128	6298	3391
"	2-4	7063	1850	8350	3937	7000	9900	196	119	89	63	6100	3850
"	4-6	6944	1884	8085	4712	6547	7738	182	106	99	191	5853	3571
"	6-8	6484	1800	7881	3741	6883	11372	179	114	90	36	5786	3591
"	8-10	5596	1710	8551	4149	6539	8551	188	124	111	25	8048	3521
"	10-12	5688	1700	8600	4187	7000	11900	185	125	106	40	6700	3900
"	12-15	5813	1750	9351	4688	6701	8601	177	119	105	66	7502	3951
"	15-20	5311	1900	8498	3718	6698	9898	176	138	110	38	7998	3899
"	20-25	4709	1657	8388	4206	6329	8438	147	121	110	24	6631	3415
G(B')951	0-2	6979	1559	6589	4338	5734	8551	169	92	94	25	5375	3219
"	2-4	6632	1702	6958	4317	6207	11313	686	390	135	130	19022	3755
"	4-6	5124	950	5749	3124	5199	8498	149	85	81	48	5099	292
"	6-8	6376	1600	6451	3750	6101	10602	161	85	86	40	5201	3200
"	8-10	5625	1300	6350	4125	7000	7900	135	74	90	20	4700	2900
"	10-12	5688	1400	6050	4000	5800	9100	113	59	87	26	3850	2950
"	12-15	4427	911	6627	3510	6577	9309	136	70	91	18	4908	7682
"	15-20	5410	1549	7497	4466	7596	10195	155	93	96	65	5398	3199
"	20-25	4866	1547	6538	3961	6488	10106	164	114	106	23	6788	3693
"	25-30	5063	1700	7800	3875	6300	11000	154	109	108	21	6350	4000
"	30-35	4058	1598	10289	4276	7292	9590	151	135	124	23	7992	3996
"	35-37	4358	1494	8517	4233	6276	9762	131	127	117	23	6974	3935

Table XVI-3   Average major oxide ratios of the insoluble fraction of pelagic sediment from the Central Pacific Basin (this study), DOMES sites (PIPER et al., 1979) and of terrigenous shale (TUREKIAN and WEDEPOHL, 1961). The samples are arranged left-to-right in order of relative location from west to east. See Fig. XVI-1 for their actual location.

	Central Pacific Basin	DOMES Site A	DOMES Site B	DOMES Site C	Shale
Fe_2O_3/Al_2O_3	0.608	.517	.471	.457	0.446
MgO/Al_2O_3	.205	.173	.166	.156	0.164
CaO/Al_2O_3	.065	.058	.050	.042	0.204
Na_2O/Al_2O_3	.0640	.0813	.0872	.0850	0.0851
K_2O/Al_2O_3	0.184	.165	.180	.192	0.211
TiO_2/Al_2O_3	.072	.057	.055	.053	0.051
P_2O_5/Al_2O_3	.0058	.0073	.0066	.0055	0.001
MnO/Al_2O_3	.0054	.0043	.0040	.0037	0.0073
SiO_2/Al_2O_3	5.39	4.52	4.55	3.57	3.86

Table XVI-4   Concentrations of biogenic $CaCO_3$ and SiO_2 calculated from bulk compositions (Table XVI-1). Refer to the text for the procedure.

	P138 (0–2)	P138 (6–8)	P138 (15–17)	P138 (163–165)	P138 (378–380)	G(B')948 (0–2)	G(B')948 (6–8)	G(B')948 (13–15)
$CaCO_3$	1.91	2.00	1.90	8.14	20.87	1.60	1.74	1.53
SiO_2	9.75	6.23	9.15	10.31	31.84	11.79	10.36	7.73

	G(B')948 (28–30)	G(B)950 (0–2)	G(B')951 (0–2)	G(B')951 (4–6)	G(B')951 (8–10)	G(B')951 (13–15)	G(B')951 (23–25)
$CaCO_3$	1.48	1.87	1.46	1.31	1.34	1.41	1.93
SiO_2	1.26	11.05	14.14	16.25	10.00	14.33	6.33

east-west line between 8° and 15°N. At each site (Fig. XVI-1) the composition of the ISF is uniform. The composition of this sediment fraction for the Central Pacific Basin compares closely with the ISF of the other three areas in the North Pacific (Table XVI-3). Sample P138 (378–380)R from the Central Pacific, however, is significantly different (Table XVI-1) from the other samples with regard to its $CaO:Al_2O_3$ and $TiO_2:Al_2O_3$ ratios.

Between the four sites, compositional ratios exhibit a longitudinal trend. This east-west trend in the composition of the ISF may be related to a decreasing influence of continentally derived material from east to west. The ISF at DOMES Site C, the easternmost of these four locations, most closely resembles the composition of terrigenous mud. An increase in the relative contribution of basaltic debris, from east to west, may be one factor contributing to the relative increases of Fe_2O_3, MgO, CaO, and TiO_2 and the decrease in total alkalies along this same trend.

Certainly other factors, such as sediment diagenesis and clay mineralogy, contribute in a major way to variations in sediment composition. For the DOMES samples, the concentration of montmorillonite in the clay-size fraction correlates strongly with the trends in elemental composition (PIPER et al., 1979). This correlation and the elemental composition of sediment from the Central Pacific Basin suggests that the concentration of montmorillonite in the samples of this study is about 30%.

Soluble Sediment Fraction (SSF)

The soluble sediment fraction consists of amorphous metal oxides (predominantly Fe^{+3}, Mn^{+4}, and possibly Al^{+3}), adsorbed ions (Na^+, K^+, Ca^{++}, and Mg^{++}), $CaCO_3$, and manganese nodules. Within the fine fraction of sediment, minor metals (Ni, Cu, Co and Zn) have been found in similar studies to correlate strongly with Mn, suggesting that they also occur in the amorphous oxide fraction.

The distribution of this fine-grained fraction and its variations in composition may have particular relevance to the genesis of manganese nodules. Basically, two types of nodules can be distinguished in the North Pacific by their mineralogy (CALVERT and PRICE, 1977), surface texture (PIPER et al., 1979) and elemental composition. Nodules with relatively high Ni:Mn and Cu:Mn ratios contain todorokite as a major mineral and have a granular surface texture. The second group has relatively low Ni:Mn and Cu:Mn ratios, exhibits a smooth surface texture, and contains little todorokite. This latter group of nodules is considered to receive most of its metal content directly from the overlying seawater, whereas the nodules containing todorokite receive a large contribution of metals from the interstitial water of associated sediment during sediment diagenesis.

This interpretation implies that sediments lose relatively more Cu and Ni than Mn to nodules during diagenesis and that the Cu:Mn and Ni:Mn ratios decrease with depth in the sediment. In the three box cores the Cu:Mn ratio decreases with depth in the sediment (Fig. XVI-2). The Ni:Mn ratio is more variable. In all three box cores it displays an indistinct minimum between approximately 10 and 15 cm depth (Fig. XVI-2). In box core G(B')951 the Ni:Mn ratio has a subsurface maximum above this minimum. The absolute concentrations of each metal in the three box cores are approximately the same. The Mn:Co ratio does not vary significantly. The distribution of Zn shows considerable scatter.

A surprisingly large fraction of the Al is also present in the SSF, approximately 10% of the total Al. Profiles of absolute concentration exhibit considerable scatter. Variable dilution of the hydrogenous component by biogenic material, mostly opaline silica, may account for much of this scatter. When normalized to soluble Mn, however, the Al profiles show a curve similar to those of Cu:Mn ratios.

References

CALVERT, S. E. and PRICE, N. B. (1977) Geochemical variation in ferromanganese nodules and associated sediments from the Pacific Ocean. *Mar. Chem.*, vol. 5, p. 43-74.

CHESTER, R. and HUGHES, M. I. (1967) A chemical technique for the separation of ferromanganese minerals, carbonate minerals, and adsorbed trace elements from pelagic sediment. *Chem. Geol.*, vol. 2, p. 249-262.

GOLDBERG, E. D. (1963) Mineralogy and chemistry of marine sedimentation, *In* SHEPARD, F. P. (ed.), *Submarine Geology*, New York, Harper and Row, p. 436-466.

PIPER, D. Z., LEONG, K., and CANNON, W. F. (1979) Manganese nodule and surface sediment compositions: DOMES Sites A, B, and C. *In* BISCHOFF, J. L. and PIPER, D. Z. (eds.), *Marine Geology and Oceanography of the Pacific Manganese*
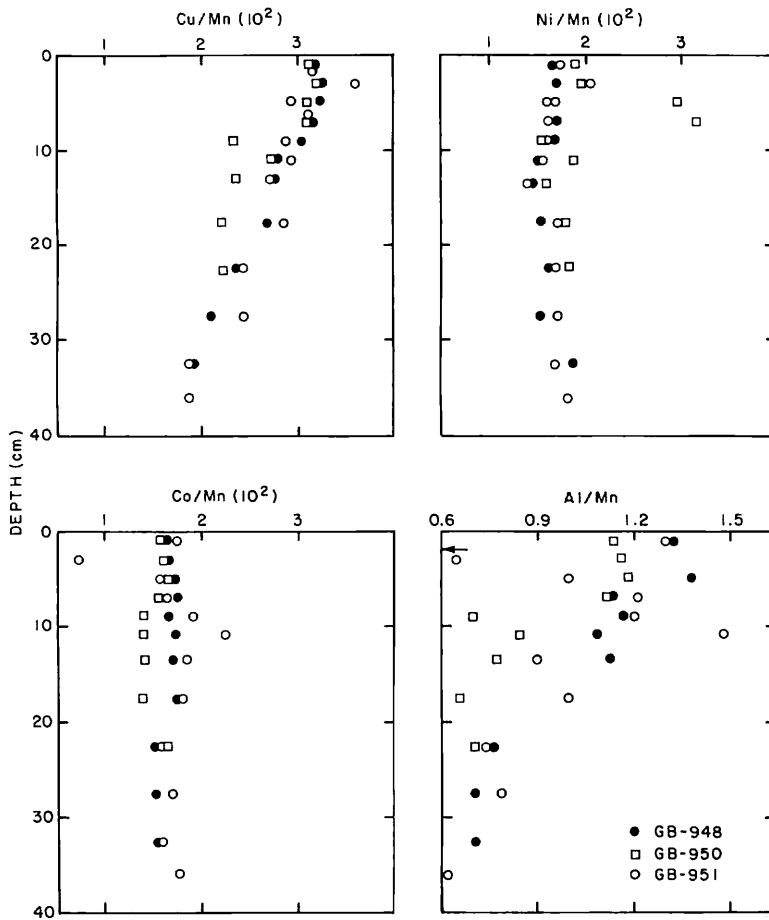
Fig. XVI-2 Sediment profiles for metals within the SSF (Table XVI-2) of three box cores.

Nodule Province, Plenum Publ. Corp., New York, p. 437–473.

TUREKIAN, K. K. and WEDEPOHL, K. H. (1961) Distribution of the elements in some major units of the earth's crust. *Geol. Soc. Amer. Bull.*, vol. 72, p. 175–192.